



**UNIVERSITY OF LEEDS**

This is a repository copy of *Assessment of semi-mechanistic bubble departure diameter modelling for the CFD simulation of boiling flows*.

White Rose Research Online URL for this paper:  
<http://eprints.whiterose.ac.uk/141799/>

Version: Accepted Version

---

**Article:**

Colombo, M, Thakrar, R, Fairweather, M et al. (1 more author) (2019) Assessment of semi-mechanistic bubble departure diameter modelling for the CFD simulation of boiling flows. *Nuclear Engineering and Design*, 344. pp. 15-27. ISSN 0029-5493

<https://doi.org/10.1016/j.nucengdes.2019.01.014>

---

© 2019 Elsevier B.V. All rights reserved. Licensed under the Creative Commons Attribution-Non Commercial No Derivatives 4.0 International License (<https://creativecommons.org/licenses/by-nc-nd/4.0/>).

**Reuse**

This article is distributed under the terms of the Creative Commons Attribution-NonCommercial-NoDerivs (CC BY-NC-ND) licence. This licence only allows you to download this work and share it with others as long as you credit the authors, but you can't change the article in any way or use it commercially. More information and the full terms of the licence here: <https://creativecommons.org/licenses/>

**Takedown**

If you consider content in White Rose Research Online to be in breach of UK law, please notify us by emailing [eprints@whiterose.ac.uk](mailto:eprints@whiterose.ac.uk) including the URL of the record and the reason for the withdrawal request.



[eprints@whiterose.ac.uk](mailto:eprints@whiterose.ac.uk)  
<https://eprints.whiterose.ac.uk/>

# **Assessment of semi-mechanistic bubble departure diameter modelling for the CFD simulation of boiling flows**

**Marco Colombo\*<sup>1</sup>, Ronak Thakrar<sup>2</sup>, Michael Fairweather<sup>1</sup> and Simon P. Walker<sup>2</sup>**

<sup>1</sup> School of Chemical and Process Engineering  
University of Leeds, Leeds, LS2 9JT, United Kingdom

<sup>2</sup> Department of Mechanical Engineering, Imperial College London, Exhibition Road, London, SW7 2AZ, United Kingdom

\* Corresponding Author: M.Colombo@leeds.ac.uk; +44 (0) 113 343 2351

## **ABSTRACT**

Eulerian-Eulerian two-fluid computational fluid dynamic (CFD) models are increasingly applied to predict multiphase and boiling flows in nuclear reactor thermal hydraulics. In these models, nucleate boiling is usually accounted for by partitioning the heat flux between the different mechanisms of heat transfer involved. Although structured in a mechanistic fashion, heat flux partitioning models are still forced to rely on mainly empirical closure relations. Between the numerous closures required, the bubble departure diameter in particular has a significant influence on the predicted interfacial area concentration and void distribution within the flow. There is now abundant evidence in the literature of the limited accuracy and reliability of the empirically-based correlations that are normally applied in CFD models. In view of this, in this work more mechanistic formulations of bubble departure have been introduced into the STAR-CCM+ code. The models are based on a balance of the hydrodynamic forces that act on a bubble at the nucleation site. Their performance, and compatibility with existing implementations in a CFD framework, are assessed against two different data sets for vertically upward subcooled boiling flows. In general, a significant number of modelling choices is required by these mechanistic models and some recommendations are made. The models are extended to include a more physically-consistent coupled calculation of the frequency of bubble departure. In general, predictions of the wall temperature reach a satisfactory accuracy, even if numerous numerical and modelling uncertainties are still present. In view of this, several areas for future work and modelling improvement are identified, such as the proper modelling of the local subcooling acting on the bubble cap.

## **KEYWORDS**

Nucleate boiling, computational fluid dynamics, bubble departure diameter, semi-mechanistic model

## **1. INTRODUCTION**

Boiling is a very efficient heat transfer mechanism and the convenience of transferring large amounts of heat with minimum temperature differences is exploited in numerous industrial and engineering sectors. Practically all water-cooled nuclear reactors experience some degree of boiling, during the normal operation of the plant or in design-basis and beyond design-basis postulated accidents. However, the physics of boiling and the mechanisms triggering a boiling crisis (often referred to as the departure from nucleate boiling (DNB) or dryout), still lack robust and reliable modelling and comprehensive understanding (Bestion, 2012; Yadigaroglu, 2014). In recent years, computational fluid dynamics (CFD) has proved of value in the prediction of multiphase flows and multiphase nuclear reactor thermal hydraulics. CFD can capture physical processes across large ranges of length scales and with finer spatial and temporal resolution than conventional 'system code based' thermal hydraulic approaches. Therefore, CFD methods are appealing for the prediction of boiling and the critical heat flux, which is the maximum amount of heat that is safely transferrable before triggering the boiling crisis.

In recent years, many attempts have been made to incorporate wall boiling models into CFD codes and specifically in the two-fluid models that are most often used to tackle component-scale engineering problems. Most commercial CFD platforms include inside their two-fluid averaged models some boiling capability that is typically based on the Rensselaer Polytechnic Institute (RPI) heat flux partitioning model introduced by Kurul and Podowski (1990). In this model, the heat flux from the wall is partitioned between the mechanisms that are presumed to be responsible for the heat transfer process; single-phase convection, quenching and evaporation. Although the RPI model and all its more recent modifications are structured in a mechanistic fashion, they rely on numerous mostly empirical or semi-empirical closure relations (Krepper and Rzehak, 2011; Koncar and Matkovic, 2012; Thakrar et al., 2017). The evaporative heat transfer component, in particular, requires closures for the active nucleation site density, the bubble departure diameter and the bubble departure frequency to calculate the rate of phase

change at the wall. In most CFD studies to date, these have been predicted with different empirical correlations. The numerous correlations available have been reviewed in Thakrar et al. (2014) and Cheung et al. (2014) and were found in both studies to usually have limited accuracy and generality. The wider applicability of the RPI model is thus limited and calibration has been often required to accurately predict boiling flow data sets under investigation (Yeoh and Tu, 2006; Krepper et al., 2013; Colombo and Fairweather, 2016a). It is therefore expected that the predictive capability of the RPI model can be improved by gradually replacing the current mostly empirical closures in favour of more mechanistic sub-modelling.

This paper investigates the semi-mechanistic modelling of the bubble departure diameter closure. In the RPI model, the value of the departure diameter is required to calculate the evaporative heat flux and the portion of the wall surface where boiling is the dominant heat transfer mechanism. In addition, the bubble departure diameter determines the wall nucleation source in population balance models. These are normally coupled to the two-fluid framework and track the evolution of the bubble diameter distribution in the flow (Yao and Morel, 2004; Yun et al., 2012; Colombo and Fairweather, 2016a). Therefore, the accuracy of this particular closure has a large impact upon predicted mean flow quantities, including the void fraction distribution and the temperature field in the liquid.

In recent decades, more mechanistic approaches for predicting the departure diameter under pool and forced convective boiling conditions have been proposed. These originate from the model of Klausner et al. (1993). In this model, bubble growth is computed from an approach based on the diffusion of heat into the bubble from the surrounding liquid. Detachment of the bubble from the nucleation cavity is evaluated from a balance of the hydrodynamic forces that act on the bubble. The model, validated against measurements in refrigerant R113 under saturated boiling conditions, was later extended to both pool and flow boiling (Zeng et al., 1993a; Zeng et al., 1993b). Over the years, subsequent modelling efforts have largely attempted to calibrate Klausner et al.'s model to extend its predictive capability to cover a wider range of experimental conditions (Situ et al., 2005; Wu et al., 2008). Sgrue and Buongiorno (2016) calibrated Klausner et al.'s model against several low-pressure data sets by making adjustments to the contact diameter model. Other authors have included additional heat transfer mechanisms to the

existing models, mainly based on the growth of a bubble in an infinite uniformly superheated liquid (Forster and Zuber, 1954; Plesset and Zwick, 1954). Yun et al. (2012) introduced the effect of local condensation into the bubble growth rate model and suggested modifications to both the lift force and the surface tension models. Colombo and Fairweather (2015) extended Yun et al.'s (2012) model by including the contribution of microlayer evaporation beneath the bubble based on the approach of Cooper and Lloyd (1969). The same microlayer model, with a modified growth equation to account for local condensation on the bubble cap, was recently applied by Mazzocco et al. (2018). Whilst these models continue to incorporate a significant empirical component, it is hoped nevertheless that the more local considerations involved will extrapolate more effectively toward high-pressure pressurized water reactor (PWR) conditions, where measurements of diameter are scarce for obvious reasons.

Overall, these models have rarely been implemented inside CFD codes (Yun et al., 2012; Yeoh et al., 2014; Gilman and Baglietto, 2017). Even less frequent have been analyses focused on the force-balance model itself, particularly in relation to the local near-wall flow conditions that are required as input, normally at a length scale smaller than the first near-wall finite-volume cell, in particular at high pressure. Recently, Thakrar and Walker (2016) undertook an evaluation of the force-balance model of Sugrue and Buongiorno (2016) in the STAR-CCM+ commercial code (CD-adapco, 2016). Authors were able to predict reasonably well the popular high pressure subcooled boiling test case of Bartolomei and Chanturiya (1967), most computations of this test case having used a bubble departure diameter obtained from empirical correlations. Amongst numerous options, correlations from Tolubinsky and Kostanchuk (1970) and Kocamustafaogullari (1983) are frequently used. Being derived from mean parametric data, these are not, however, equipped to reflect the dependency on the local flow conditions that are normally available in a CFD calculation (Thakrar and Walker, 2016).

In this work, three force balance models, from Klausner et al. (1993), Yun et al. (2012) and Sugrue and Buongiorno (2016), are implemented in the STAR-CCM+ code (CD-adapco, 2016). The performance of the CFD model is assessed blindly against the experiments of Bartolomei and Chanturiya (1967) and Garnier et al. (2001) (referred to more commonly as the DEBORA benchmark) for subcooled boiling flows of water and refrigerant in vertical pipes. Although not

entirely similar, these experiments were selected to replicate as closely as possible elevated pressure operating conditions in PWRs. Results are also compared with the most frequently used empirical correlations. Impacts on the results of different modelling choices are examined and results of the force balance analyzed and possible improvements in the modelling of some forces are suggested. Bubble departure frequency is also directly evaluated from the force balance model, improving the internal physical consistency of the model. Finally, some sensitivity studies are made on the modelling of condensation on the bubble cap.

## 2. EXPERIMENTAL DATA

Two experiments have been predicted in this work, from the database of Bartolomei and Chanturiya (1967) and the DEBORA experiment (Garnier et al., 2001), with the specific conditions considered reported in Table 1.

Table 1. Experimental conditions of the two test cases.

Experiment	p [MPa]	G [kg m <sup>-2</sup> s <sup>-1</sup> ]	q [kWm <sup>-2</sup> ]	T <sub>in</sub> [°C]	D [m]	Fluid
Bartolomei and Chanturiya	4.5	900	570	197.4	0.0154	Water
DEBORA	2.62	1985	73.9	70.5	0.0192	R12

Bartolomei and Chanturiya (1967) investigated the subcooled boiling of water flowing upward in a vertical pipe of inner diameter  $D = 0.0154$  m and length  $L = 2$  m. Area-averaged void fractions were measured using a gamma-ray attenuation technique driven by a Thulium-170 source at different axial locations and at pressures up to 15 MPa, mass fluxes up to 2000 kg m<sup>-2</sup> s<sup>-1</sup> and heat fluxes up to 2.2 MW m<sup>-2</sup>. In addition, wall temperature, axial liquid temperature and area-averaged liquid temperature measurements were also provided for the 4.5 MPa case, and, therefore, this specific experiment is simulated here.

The DEBORA (Garnier et al., 2001) flow loop consisted of a 19.2 mm inner diameter vertical pipe, heated for a length of 3.5 m and operated with Freon-12 (R-12). It is both difficult and expensive to measure the flow boiling behaviour of water at high pressure. Employing R-12 as the working fluid partially replicates the flow characteristics of a prototypical high pressure flow of water under much milder conditions. In the range of pressures investigated in the DEBORA experiment (1.46 – 3.01 MPa), the values of the relevant dimensionless groups for R-12, such as

the Reynolds and Weber numbers, and the density ratio, are comparable to those found in PWRs. Void fraction and vapour velocity profiles at the end of the test section were measured with an optical probe technique, from which radial profiles of the interfacial area concentration and the Sauter mean diameter (SMD) were determined. Thermocouples were used to measure the liquid temperature radial profile and the wall temperature at selected axial locations. Details of the specific experiment investigated here, characterized by a pressure of 2.62 MPa, are given in Table I.

Measurements of the bubble departure diameter are not provided by either of the two experiments. Such measurements, particularly under forced convective conditions, are understandably quite scarce at elevated pressure. Similarly, data for mean flow quantities under prototypic reactor operating conditions ( $\sim 15$  MPa) is equally scarce. The two databases selected are amongst the most frequently employed for validating CFD boiling predictive capability, and represent an appropriate compromise between data availability and proximity to true nuclear reactor operating conditions.

### **3. MATHEMATICAL MODEL**

In a two-fluid Eulerian-Eulerian model, each phase is described by a set of time averaged conservation equations, and the continuity, momentum and energy equations are solved for each phase. These are discussed in many previous publications, such as Ishii and Hibiki (2006), and are not presented here. Instead, the description is focused on the wall boiling and the bubble departure diameter models, these being the main subject of the work. Implementation of all the other models follows a standard approach and a full description of the models as well as the values of the many modelling parameters employed can be found in CD-adapco (2016). The drag model of Tomiyama et al. (1998) is used with the model of Burns et al. (2004) for the turbulent dispersion. Lift and wall lubrication forces are not included. Although both might affect boiling modelling, their role and magnitude in boiling flows is not well-understood and unlikely to be predicted with accuracy by models designed for adiabatic bubbly flows. A standard high-Reynolds multiphase version of the  $k$ - $\varepsilon$  turbulence model (Jones and Launder, 1972) solves for the turbulence in the liquid phase, whereas in the vapour phase the turbulence is directly related

to that in the liquid using a turbulence response model (in this case with the turbulence in both phases being equal).

Bubbles, after their departure from the heated wall, experience evaporation and condensation in the bulk of the flow, and break-up and coalescence events that alter the bubble diameter distribution and affect the interphase mass, momentum and energy exchanges. The bubble diameter distribution is predicted with the  $S_\gamma$  model (Lo and Zhang, 2009). Moments of the bubble diameter distribution, which is assumed to obey to a pre-defined log-normal shape, are calculated and used to define the SMD in the flow:

$$S_\gamma = nM_\gamma = n \int_0^\infty d_B^\gamma P(d_B) d(d_B) \quad (1)$$

The one-equation version of the model is considered (CD-adapco, 2016) and the transport equation for the second moment of the bubble distribution is solved to find the SMD:

$$\frac{\partial S_\gamma}{\partial t} + \nabla \cdot (S_\gamma \mathbf{U}_v) = S_{br}^\gamma + S_{cl}^\gamma \quad (2)$$

$$d_{SM} = d_{32} = \frac{S_3}{S_2} = \frac{6\alpha}{a_i} \quad (3)$$

Breakup and coalescence models are taken from Yao and Morel (2004) and adapted following the work of Colombo and Fairweather (2016b), where they were successfully validated against air-water bubbly flows. Here, a value of 1.24 is used for the critical Weber number  $We_{cr}$ . Finally, condensation and evaporation in the bulk of the fluid are evaluated from the Ranz and Marshall (1952) correlation.

### 3.1 Wall Heat Flux Partitioning Model

When nucleate boiling takes place at the wall, wall superheat and the related heat transfer coefficient, and the temperature in the wall-adjacent finite-volume cell, are obtained from the solution of the wall heat flux partitioning model. Following the RPI approach, the total heat flux is partitioned between the mechanisms responsible for heat removal:

$$q_w = (q_l + q_q + q_{ev})(1 - K_{dry}) + K_{dry}q_v \quad (4)$$



Latent heat is removed by evaporation ( $q_{ev}$ ) and supports the growth of vapour bubbles at the active nucleation sites. Detachment of these bubbles promotes additional mixing by drawing in cooler liquid in the space previously occupied by the bubble, causing rewetting of the heating surface, and this additional contribution to the total heat transfer ( $q_q$ ) is often referred to as quenching. In regions of the wall not affected by boiling, sensible heat is transferred to the liquid-phase by ordinary single-phase convection ( $q_l$ ). Finally, if the amount of vapour generated at the wall is high enough so as to begin to obstruct surface rewetting, a portion of the wall heat is transferred by convection to the vapour phase ( $q_v$ ). In this case, the fraction of the wall surface in contact with the vapour phase is represented by  $K_{dry}$ , which becomes larger than zero when the void fraction is higher than a critical value, assumed equal to 0.9. The heat flux for the single-phase convective contribution is evaluated using standard wall treatments and using the temperature in the near-wall cell  $T_l$ , as illustrated below:

$$q_l = (1 - A_b)h_l(T_w - T_l) = (1 - A_b)\frac{\rho_l C_{p,l} u_{\tau,l}}{T_l^+} (T_w - T_l) \quad (5)$$

The boiling area fraction  $A_b$  is the fraction of the wall affected by the evaporation process and  $T_l^+$  is the dimensionless temperature in the near-wall cell. The convective heat flux to the vapour phase is calculated in a similar way. The quenching heat flux is expressed as the product of a quenching heat transfer coefficient, modelled as a transient conduction into a semi-infinite medium (Del Valle and Kenning, 1985), and the temperature difference between the wall and the liquid:

$$q_q = A_b h_q (T_w - T_l) = 2A_b f \sqrt{\frac{\rho_l C_{p,l} \lambda_l t_w}{\pi}} (T_w - T_l) \quad (6)$$

In the previous equation, the waiting time  $t_w$  is equal to 80 % of the total ebullition cycle of a bubble, known from the inverse of the bubble departure frequency  $f$ , and, to avoid any dependency on the computational grid, the liquid temperature is evaluated at a constant wall  $y^+$  of 250. The evaporative heat flux is known from the mass flux of bubbles generated at the wall and the latent heat of vaporization  $i_h$ . Assuming the bubbles are spherical, this mass flux is easily

computed from the number of nucleation sites active per unit area  $N_A$ , the bubble departure diameter  $d_{dep}$  and the bubble departure frequency  $f$ :

$$q_{ev} = N_A f \left( \frac{\pi d_{dep}^3}{6} \right) \rho_v i_{lv} \quad (7)$$

The nucleation site density and bubble departure diameter are also used to derive the fraction of the wall exposed to the boiling process:

$$A_b = 2.0 \frac{\pi d_{dep}^2}{4} N_A \quad (8)$$

It is clear that predictions of the heat flux partitioning model are strongly related to the closure models for the active nucleation site density, the bubble departure diameter and the bubble departure frequency. Normally, these are predicted using empirical closures that, being mostly derived from bulk parameters, show limited accuracy and applicability, and solutions that are frequently grid-dependent. Correlations for the active nucleation site density in particular are associated with significant uncertainty related to the specific conditions of the surface. This is not addressed in the present paper and the site density is predicted using the correlation of Hibiki and Ishii (2006), which has been shown to give a  $\sim 50\%$  error for high pressure water flows.

The bubble departure diameter is calculated from a force balance approach. More specifically, bubble growth is predicted from an energy balance that accounts for the different mechanisms of heat transfer between the bubble and the wall, and the surrounding liquid. The departure condition is evaluated from balances of the forces acting on the bubble in directions parallel ( $x$ ) and perpendicular ( $y$ ) to the heated wall. Depending on the balance that is violated first, therefore, the departure diameter used by the heat flux partitioning model is the diameter at which the bubble departs (parallel) and begins to slide away from the nucleation site and along the wall, or lifts-off (perpendicular), moving away from the wall and towards the bulk of the flow. The much greater heat fluxes required to drive boiling at elevated pressures cause bubbles to lift-off very quickly (Thakrar and Walker, 2016). It is thus reasonable to assume that bubbles lift-off immediately following departure at the conditions investigated here.

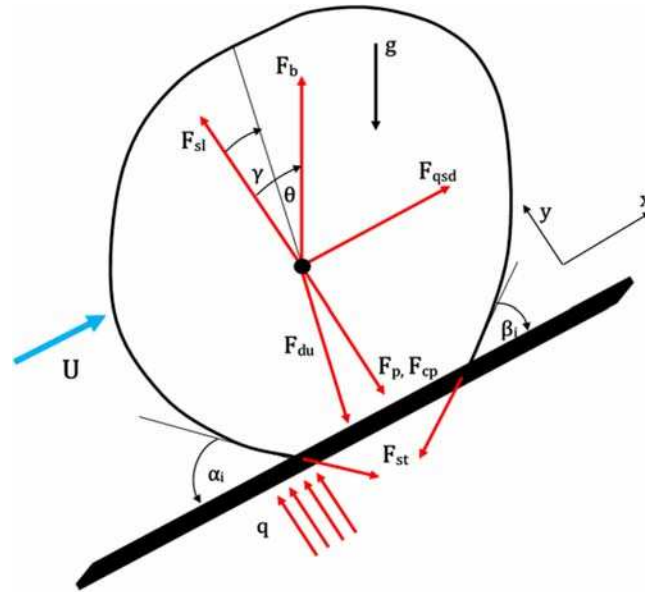


**Figure 1. Forces acting on a bubble at the nucleation site.**

The three force balance models from Klausner et al. (1993), Yun et al. (2012) and Sugrue and Buongiorno (2016) were applied. As discussed previously, the latter two are extensions of the former, which was developed and validated against flow boiling of R113 in a square duct at atmospheric pressure. Specifically, instead of the constant contact diameter  $d_w$  employed by Klausner et al. (1993), both introduced a variable value calculated as a fraction of the bubble diameter. Sugrue and Buongiorno (2016) employed  $d_w / d_B = 0.025$ , while the value 0.067 was adopted by Yun et al. (2012). The force balance considers several forces: the surface tension force  $F_{stx/sty}$  that keeps the bubble attached to the wall; the buoyancy force  $F_b$  that promotes the departure of the lower density bubble; the quasi-steady drag force  $F_{qs}$  and the shear lift force  $F_{sl}$ , quantifying the tendency of the fluid flow to strip the bubble from the nucleation site; the unsteady drag force due to asymmetrical bubble growth  $F_{dux/duy}$ , representing the opposition to bubble growth exercised by the fluid that surrounds the bubble; and the pressure forces over the bubble surface, split between the hydrodynamic force  $F_p$  and the contact pressure force  $F_{cp}$  (see Figure 1). No additional modifications to these forces have been introduced, although their applicability to the conditions investigated is still unclear and, inevitably, the modelling still relies on a number of empirical parameters. Between these parameters, the only small difference is the value of the shear lift coefficient  $C_l$  that Yun et al. (2012) fix at 0.118, higher than both Klausner et al. (1993) and Sugrue and Buongiorno (2016). For both the Klausner et al. (1993) and Sugrue and Buongiorno (2016) models, the bubble growth equation from Forster and Zuber

(1954) with a value of  $b = 1.56$  is used, this being the asymptotic solution of the Mikic and Rohsenow (1969) model that was originally adopted by Klausner et al. (1993). A similar modification to the original Klausner et al. (1993) model was introduced in the subsequent paper from Zeng et al. (1993a). Instead, Yun et al. (2012) added to the Forster and Zuber (1954) growth equation the contribution of the locally subcooled flow, and the condensation heat transfer coefficient was evaluated using the Ranz and Marshall (1952) model. In the results section, predictions of the three models are also compared with the widely applied correlations of Tolubinsky and Kostanchuk (1970) and Kocamustafaogullari (1983). Details of all the models adopted, the force balance and the growth equation are summarized in Table 2.

Initially, the bubble departure frequency was calculated from the correlation of Cole (1960). However, the force balance model assumes a growth rate equation, and the growth time that is derived from this may contradict the value of the departure frequency predicted using Cole's (1960) correlation. In this work, the departure frequency is obtained directly from the growth rate equation, with the growth time assumed to make up 20% of the total ebullition period (Kurul and Podowski, 1990). The results are then compared against Cole's (1960) correlation. In order to examine the impact of condensation effects, implementation of the Yun et al. (2012) force balance model is undertaken excluding in the first instance any contribution of condensation in the growth rate equation. It is worth remarking that the latter authors do not describe how the liquid temperature used in their growth rate equation is determined. Whilst this is expected to be the local temperature, indirect evidence suggests that the wall cell temperature was in fact employed. In the interests of remaining consistent with the original form of the model, similar assumptions are employed herein.

Table 2. Summary of the models for bubble departure diameter and bubble departure frequency.

Model	Form
Force balance	$\sum F_x = F_{stx} + F_{qsd} + F_b \sin \theta + F_{dux} = 0$ $\sum F_y = F_{sty} + F_{sl} + F_b \cos \theta + F_{duy} + F_p + F_{cp} = 0$ $F_{stx} = -1.25d_w\sigma \frac{\pi(\alpha_i - \beta_i)}{\pi^2 - (\alpha_i - \beta_i)^2} (\sin \alpha_i - \sin \beta_i)$ $F_{sty} = -d_w\sigma \frac{\pi}{(\alpha_i - \beta_i)} (\cos \beta_i - \cos \alpha_i)$ $F_{qsd} = 6\pi\rho_l\nu UR \left\{ \frac{2}{3} + \left[ \left( \frac{12}{Re} \right)^{0.65} + 0.862 \right]^{-1.54} \right\}$ $F_{du} = -\rho_l\pi R^2 \left( \frac{3}{2}\dot{R}^2 - R\ddot{R} \right)$ $F_b = \frac{4}{3}\pi R^3(\rho_l - \rho_v)g$ $F_{sl} = \frac{1}{2}\pi\rho_l U^2 R^2 \{ 3.877G_s^{0.5} [Re^{-2} + (C_l G_s^{0.5})^4]^{0.25} \}$ $F_p = \frac{9}{8}\rho_l U^2 \frac{\pi d_w^2}{4}$ $F_{cp} = \frac{\sigma \pi d_w^2}{R \cdot 4}$ $R(t) = \frac{2b}{\sqrt{\pi}} J a \sqrt{at}; b = 1.56$
Klausner et al. (1993)	$d_w = 0.09 \text{ mm} \quad C_l = 0.014$
Sugrue and Buongiorno (2016)	$d_w/d_b = 0.025 \quad C_l = 0.014$
Yun et al. (2012)	$d_w/d_b = 0.067 \quad C_l = 0.118$ $R(t) = \frac{2b}{\sqrt{\pi}} J a \sqrt{at} - \frac{b q_c}{S i_{lv} \rho_v} t; b = 1.56; S = 2$
Tolubinsky and Kostanchuk (1970)	$d_{dep} = d_0 \exp[-(T_{sat} - T_l)/\Delta T_0] \quad d_0 = 0.006 \text{ mm} \quad \Delta T_0 = 45 \text{ K}$
Kocamustafaogullari (1983)	$d_{dep} = d_0 \theta \left( \frac{\sigma}{g\Delta\rho} \right)^{0.5} \left( \frac{\Delta\rho}{\rho_v} \right)^{0.9} \quad d_0 = 0.0015126 \text{ mm} \quad \theta = 0.722 \text{ rad}$
Cole (1960)	$f = \sqrt{\frac{4}{3} \frac{g(\rho_l - \rho_v)}{d_{dep}\rho_l}}$
Waiting time	$t_w = 0.8/f$

### 3.2 Numerical Implementation

The overall model was solved using the steady-state solver of the STAR-CCM+ CFD code (CD-adapco, 2016). A two-dimensional axisymmetric geometry was employed and, at the inlet, a fully-developed single-phase liquid velocity, turbulence and temperature were imposed, together

with an imposed pressure at the outlet and the no-slip condition, and an imposed heat flux, at the wall. Specifically, inlet profiles were obtained, in the same geometrical domain, by performing single-phase calculations until fully-developed conditions were achieved at the same mass flow rate, with the resulting steady conditions used as initial conditions for subsequent multi-phase calculations. Constant thermophysical properties were used for both phases. More specifically, liquid properties were calculated at the average temperature between the inlet and saturation, and matched carefully against the experimental inlet mass flux. Vapour properties were calculated at saturation. A mesh sensitivity study demonstrated that grid-independent solutions (with a total number of grid elements equal to  $20 \times 375$  for the Bartolomei and Chanturiya (1967), and  $20 \times 750$  for the DEBORA, test cases) were achieved with an equidistant structured mesh that ensured the minimum wall  $y^+$  value was greater than 30, the latter being sufficiently high to justify the high-Reynolds number wall treatment selected.

#### **4. RESULTS AND DISCUSSION**

The first set of results is shown in Figures 2 and 3 for the two experiments. Predictions from the three force balance models (Klausner et al., 1993; Yun et al., 2012; Sugrue and Buongiorno, 2016), neglecting subcooling in the Yun et al. case, coupled with the Cole (1960) correlation for bubble departure frequency, are compared against wall temperature data, and predictions of the Tolubinsky and Kostanchuk (1970) and Kocamustafaogullari (1983) correlations. Bubble departure diameter predictions are generally spread over a few orders of magnitude, even if this translates into differences in the wall temperature that are limited to a 10 K range for the data in Figure 2(b) and 5 K for that in Figure 3(b).

Some issues with the Klausner et al. (1993) model are immediately apparent from Figure 2. At a certain distance from the inlet, a well-defined step is found in both the bubble departure diameter and the wall temperature. Further downstream, a solution for the lift-off diameter could not be found and the model is forced to revert back to the bubble departure solution, if available, or the default value given by the Kocamustafaogullari (1983) correlation. In contrast, upstream a solution for the lift-off diameter was successfully computed, causing the abrupt step in the value of the departure diameter. This inconsistency is related to the constant contact diameter  $d_w$  used in the Klausner et al. (1993) model, which, for the specific conditions studied, is sometimes even

higher than the bubble diameter and, therefore, prevents the code reaching an acceptable (positive) solution. Even if the same inconsistency is not found in Figure 3, a value of  $d_w$  that depends on the bubble diameter, such as that adopted by Sugrue and Buongiorno (2016) and Yun et al. (2012), is clearly preferable. Such models consistently report positive solutions for both force balances. The force balance parallel to the wall is broken first, suggesting that the bubbles may slide first before lifting off. Reasonable agreement with the Bartolomei and Chanturiya (1967) experiment is found, except in the final section of the pipe, where a sudden increase in wall temperature is predicted by both the Sugrue and Buongiorno (2016) and Yun et al. (2012) models. In the DEBORA experiment, the wall temperature is over predicted, although not excessively.

The Kocamustafaogullari (1983) correlation predicts values in the neighborhood of the force balance results. A constant value is predicted because the correlation is only a function of pressure, once the fluid properties are assumed constant with temperature. In contrast, the Tolubinsky and Kostanchuk (1970) correlation returns very high values of the bubble departure diameter and, consequently, under predicts the wall temperature. This was already observed by Thakrar and Walker (2016) for the Bartolomei and Chanturiya (1967) experiment, and confirmation is found here for the DEBORA experiment. For this reason, the Tolubinsky and Kostanchuk (1970) correlation is not used in the following comparisons. In a similar way, and in agreement with the preceding discussion, only the Sugrue and Buongiorno (2016) and Yun et al. (2012) models are considered below.

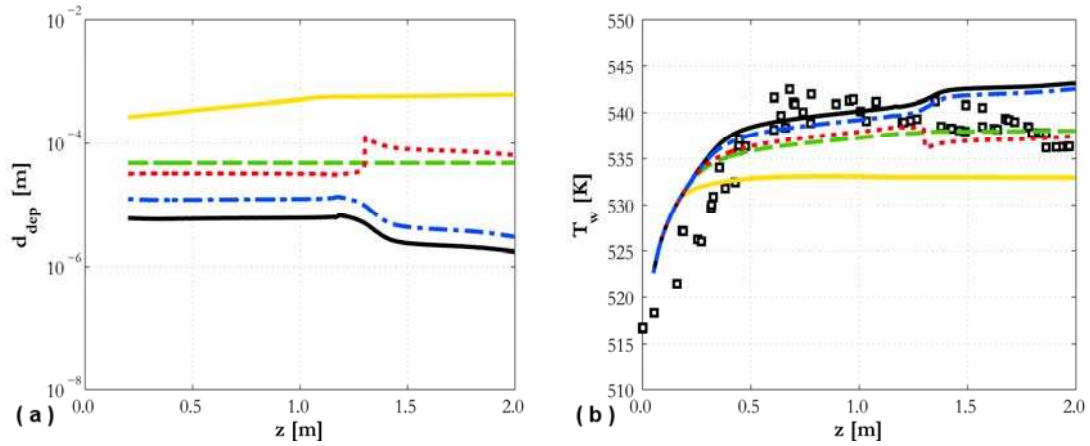


Figure 2. Predicted bubble departure diameter (a) and wall temperature (b) for Bartolomei and Chanturiya (1967) experiment: ( $\square$ ) data; (—) Tolubinsky and Kostanchuk (1970); (---) Kocamustafaogullari (1983); ( $\cdots$ ) Klausner et al. (1993); (—) Sugrue and Buongiorno (2016); (- · -) Yun et al. (2012) without subcooling. Bubble departure frequency from Cole (1960).

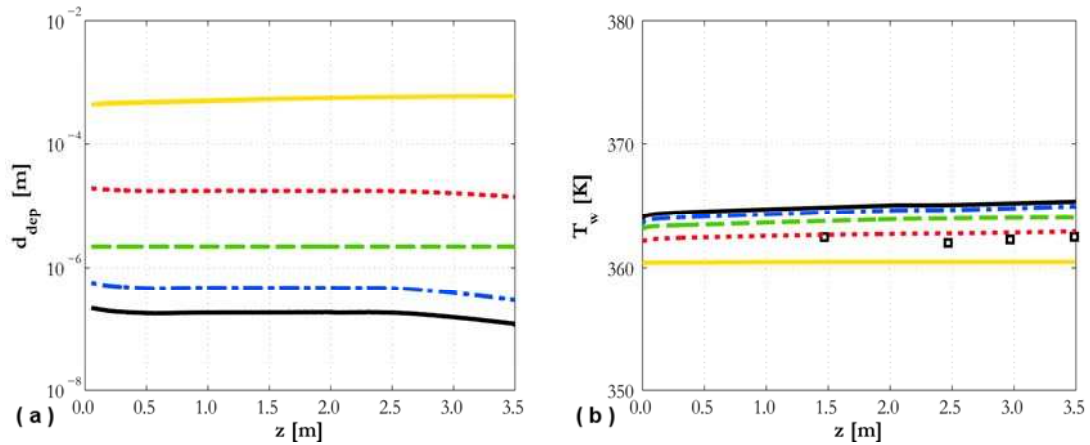


Figure 3. Predicted bubble departure diameter (a) and wall temperature (b) for DEBORA experiment (Garnier et al., 2001): ( $\square$ ) data; (—) Tolubinsky and Kostanchuk (1970); (---) Kocamustafaogullari (1983); ( $\cdots$ ) Klausner et al. (1993); (—) Sugrue and Buongiorno (2016); (- · -) Yun et al. (2012) neglecting subcooling. Bubble departure frequency is calculated from Cole (1960).

In Figures 2 and 3, the Cole (1960) model was used to predict the bubble departure frequency. In Figures 4 and 5, the bubble growth time from the departure routine was used to evaluate the frequency of bubble departure and this is compared against Cole (1960), using the Sugrue and Buongiorno (2016) bubble departure model. Clearly, using a frequency decoupled from the bubble departure diameter calculation can generate physical inconsistencies in the solution that can overcome the benefits of the more mechanistic bubble departure model. More specifically, near the end of the pipe, the departure diameter decreases (Figure 2(a)) but the frequency from



Cole (1960) remains almost constant (Figure 4(a)). This, from Eq. (7), reduces the evaporative heat flux, causing the increase in wall temperature observed in Figures 2(b) and 4(b). Using the calculated departure time, a decrease in departure diameter corresponds to a faster growth time and an increase in frequency. Therefore, the evaporative heat flux does not decrease and a flatter temperature profile is found that is more in agreement with the experiments (Figure 4(b)). Similar findings are found for the DEBORA experiment, as shown in Figure 5. A reduction in the departure diameter is reflected in a higher departure frequency and a wall temperature slightly more in agreement with experiments. Overall, the coupled departure diameter and frequency calculation improves the internal consistency of the model and the predicted frequency may differ from Cole (1960) by up to two orders of magnitude.

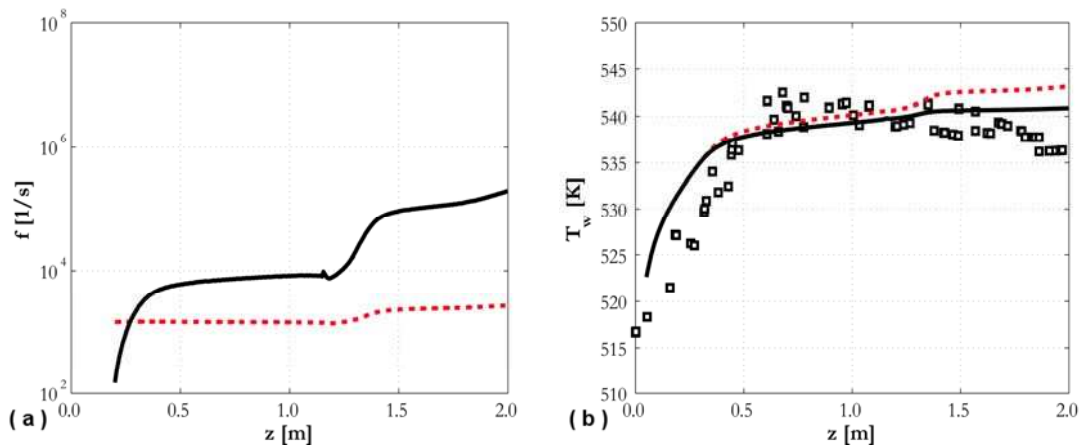


Figure 4. Predicted bubble departure frequency (a) and wall temperature (b) for Bartolomei and Chanturiya (1967) experiment using Sugrue and Buongiorno (2016) model: ( $\square$ ) data; ( $\cdots$ ) Cole (1960) model; ( $—$ ) frequency derived from departure time.

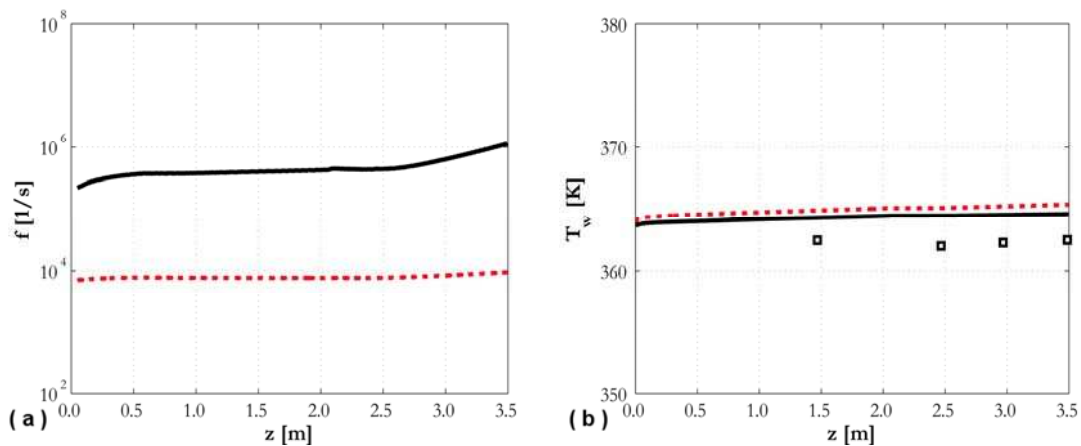
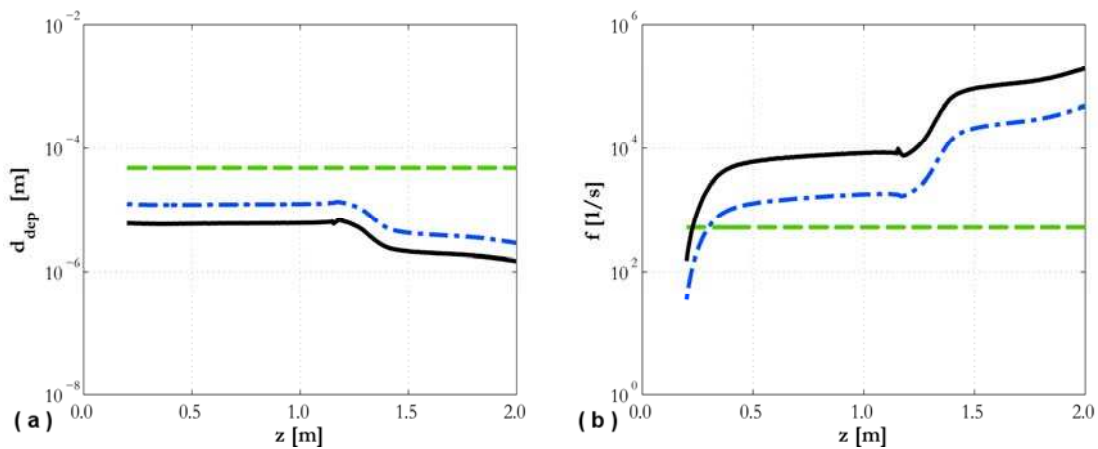


Figure 5. Predicted bubble departure frequency (a) and wall temperature (b) for DEBORA experiment (Garnier et al., 2001) using Sugrue and Buongiorno (2016) model: ( $\square$ ) data; ( $\cdots$ ) Cole

(1960) model; (—) frequency derived from departure time.

Overall comparisons of departure diameter, frequency, wall temperature and heat fluxes are reported in Figures 6 and 7. The Sugrue and Buongiorno (2016) and Yun et al. (2012) models, the latter still neglecting the subcooling contribution, return rather similar predictions, with the latter predicting a higher bubble departure diameter and lower frequency, and slightly lower wall temperature and higher evaporative heat flux. Acceptable agreement is found with wall temperature measurements, even if the observed reduction in wall temperature at the end of the pipe in the Bartolomei and Chanturiya (1967) experiment is not reproduced. This is associated indirectly with local flow acceleration in the high void fraction region, and the resulting reduction in predicted diameter under these conditions. Because the partitioning model employed does not consider the effects of coalescence, the trends illustrated are indicative of isolated boiling conditions, and do not reflect the true departure diameter in this region. In the DEBORA experiment, the wall temperature is over predicted, although not excessively. No sharp decrease in the force balance predicted departure diameter is observed downstream in the DEBORA experiment, presumably due to the much lower void fraction prediction in this experiment.



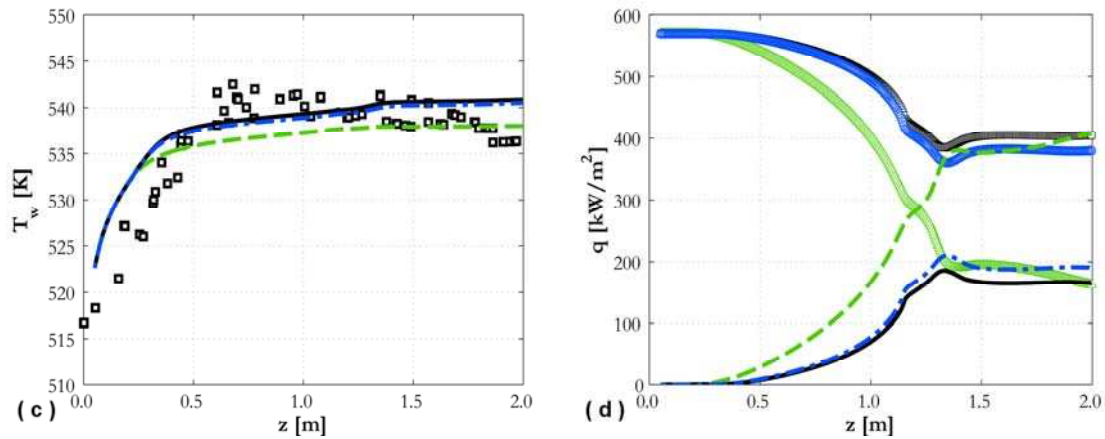


Figure 6. Predicted bubble departure diameter (a), bubble departure frequency (b), wall temperature (c) and evaporative and single-phase liquid heat fluxes (d) for Bartolomei and Chanturiya (1967) experiment: ( $\square$ ) data; (---) Kocamustafaogullari (1983); (—) Sugrue and Buongiorno (2016); (- · -) Yun et al. (2012) neglecting subcooling. In (d) lines are evaporative and symbols single-phase liquid heat fluxes: ( $\Delta$ ) Kocamustafaogullari (1983); ( $\square$ ) Sugrue and Buongiorno (2016); ( $\circ$ ) Yun et al. (2012).

An interesting trend is found in the evaporative heat flux behaviour (Figures 6(d) and 7(d)). Using the Kocamustafaogullari (1983) correlation, although the departure diameter and frequency are constant along the pipe, the evaporative heat flux increases in the outlet region, possibly because of an increase in the active nucleation site density. In contrast, the evaporative heat flux is much flatter for the two force balance models. In these, a decrease in departure diameter triggers an increase in frequency. Bubble growth is, however, modelled as only 20% of the total ebullition cycle and, therefore, the contribution of the higher departure frequency to the evaporative contribution is weakened. Therefore, further study in this area and more advanced modelling of the total ebullition cycle would be beneficial. Figures 6d and 7d also show the heat flux to the liquid phase. This includes both the convective single-phase and quenching components of the heat flux partitioning balance. Since a constant heat flux from the wall is applied in both experiments, an increased heat flux to the liquid phase corresponds to the reduced evaporative heat flux observed with the Sugrue and Buongiorno (2016) and Yun et al. (2012) models with respect to the Kocamustafaogullari (1983) approach. To accommodate this greater heat flux to the liquid phase, both the Sugrue and Buongiorno (2016) and Yun et al. (2012) models also predict a higher wall temperature.

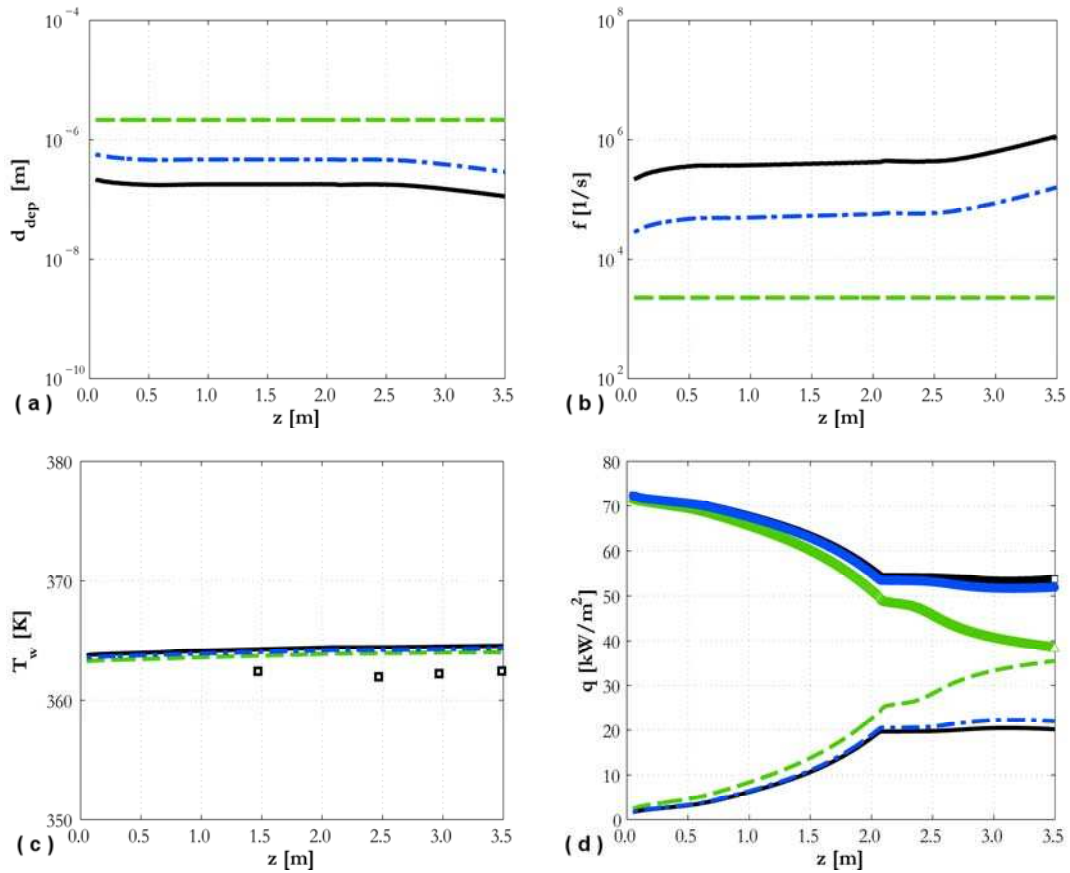


Figure 7. Predicted bubble departure diameter (a), bubble departure frequency (b), wall temperature (c) and evaporative and single-phase liquid heat fluxes (d) for DEBORA experiment (Garnier et al., 2001): ( $\square$ ) data; ( $- -$ ) Kocamustafaogullari (1983); ( $-$ ) Sugrue and Buongiorno (2016); ( $- \cdot -$ ) Yun et al. (2012) neglecting subcooling. In (d) lines are evaporative and symbols single-phase liquid heat fluxes: ( $\Delta$ ) Kocamustafaogullari (1983); ( $\square$ ) Sugrue and Buongiorno (2016); ( $\circ$ ) Yun et al. (2012).

Whereas Figure 6 and 7 were focused on wall-related quantities, comparisons for the bulk of the flow are provided in Figure 8 and 9. Figure 8 shows the average void fraction along the pipe for Bartolomei and Chanturiya (1967). The void increase along the pipe is well-predicted with the Sugrue and Buongiorno (2016), Yun et al. (2012) and Kocamustafaogullari (1983) models. In Figure 8, the model of Tolubinsky and Kostanchuck (1970) is also considered to show how an erroneous value of the bubble departure diameter can negatively affect the value of the void fraction. Specifically, the overestimated (Figure 2a) bubble departure diameter produces an excessive evaporative heat flux component. This causes the overestimation of the amount of void generated at the wall (Figure 8) and the underestimation of the wall temperature, since a reduced amount of heat needs to be accommodated by the liquid phase (Figure 2b). Comparisons against

the void fraction and average bubble diameter radial profiles for the DEBORA experiments are provided in Figure 9. The wall-peaked character of the radial void fraction profile is well-predicted (Figure 9a). This further confirms the accurate void prediction from the force balance models in the Bartolomei and Chanturiya (1967) experiment (Figure 8). More discrepancies are found in the average bubble diameter profile (Figure 9b). The increase in diameter away from the wall is well-predicted only for a portion of the radial length. Near the centre of the pipe, all the models predict a significant dip in the diameter, while the experimental profile remains flat. Similar difficulties in predicting the average bubble diameter from the DEBORA experiment were also reported in a previous paper (Colombo and Fairweather, 2016a). These results confirm that additional developments are required in the population balance model that is coupled with the boiling model. In the near wall region, all models underestimate the average diameter. However, the measurements cannot be reliably used to evaluate the accuracy of the bubble departure model. In the experiment, the bubble diameter was measured in the flow and starting from a certain distance from the wall. Even with this distance being only a fraction of a millimeter, bubble diameter at departure is still much smaller in the conditions of the experiment. Therefore, the measurements in these locations were probably already affected by interactions between the bubbles that increased the average bubble diameter but are not entirely accounted for in the overall model.

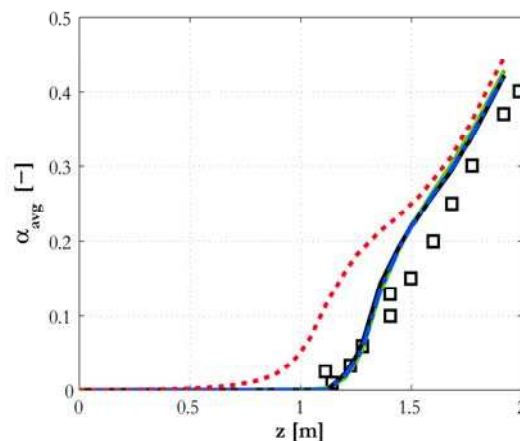


Figure 8. Area-averaged void fraction profile along the pipe in Bartolomei and Chanturiya (1967) compared against: (---) Kocamustafaogullari (1983); (—) Sugrue and Buongiorno (2016); (- · -) Yun et al. (2012); (···) Tolubinsky and Kostanchuck (1970).

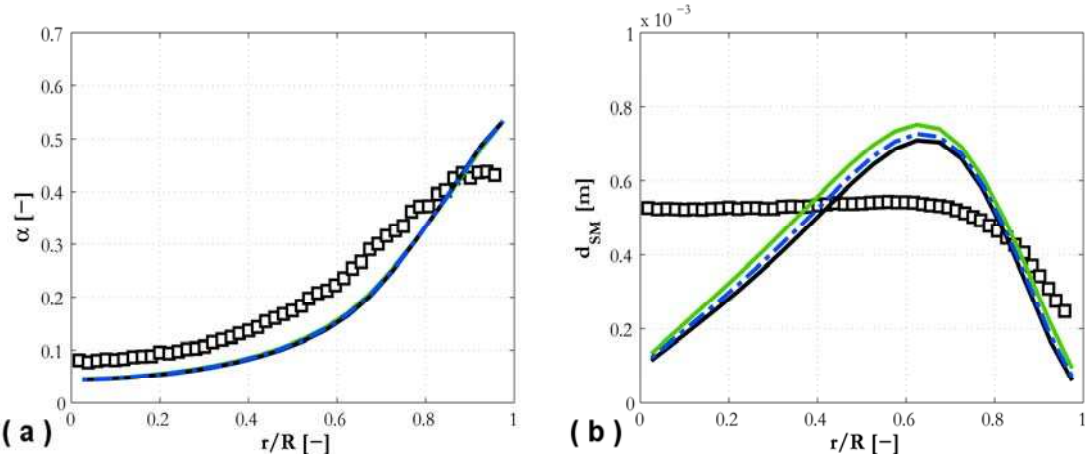


Figure 9. Void fraction (a) and averaged mean diameter (b) radial profiles from the DEBORA experiment compared against: (---) Kocamustafaogullari (1983); (—) Sugrue and Buongiorno (2016); (- · -) Yun et al. (2012).

Details of the magnitude of each force acting on a bubble can be found in Figures 10 and 11. In both experiments, the surface tension is the dominant force that keeps bubbles attached to the wall, whereas drag parallel to the wall and shear lift perpendicular to the wall promote bubble departure. Other forces are not expected to be significant, including, at these pressures, gravity. Figures 10 and 11 help to explain some of the behaviour observed previously. The magnitude of the surface tension, which is the dominant negative contribution, depends on the value of the contact diameter  $d_w$ . From Table 2, Yun at al. (2012) predicts a higher contact diameter than Sugrue and Buongiorno (2016) and, therefore, always a slightly higher bubble departure diameter in Figure 6(a) and 7(a). Klausner et al. (1993), in contrast, gives a constant value that provides results which are much higher than both of the previous models.

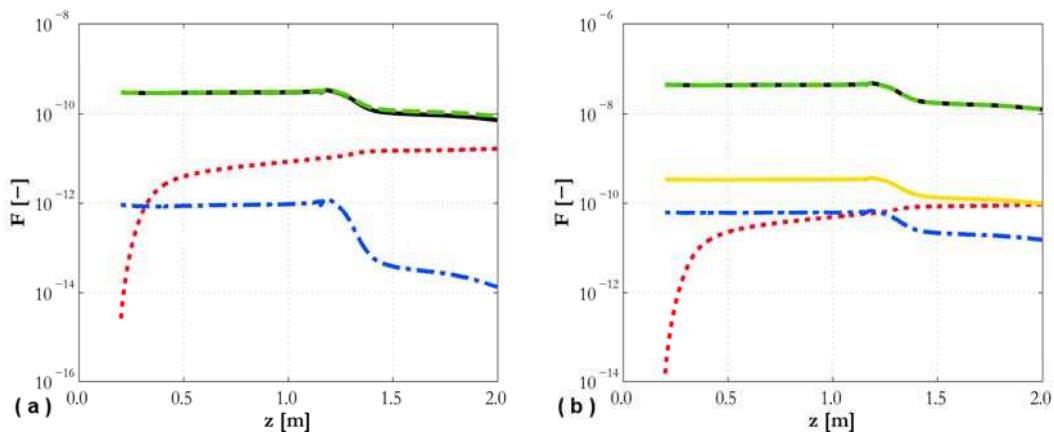


Figure 10. Contribution to force balance in wall-parallel (a) and wall-normal (b) directions for

Bartolomei and Chanturiya (1967): (—)  $F_{st}$ ; (— —)  $F_{qsd}$  (a) and  $F_{sl}$  (b); (⋯)  $F_{du}$ ; (— · —)  $F_b$  (a) and  $F_p$  (b); (—)  $F_{cp}$ .

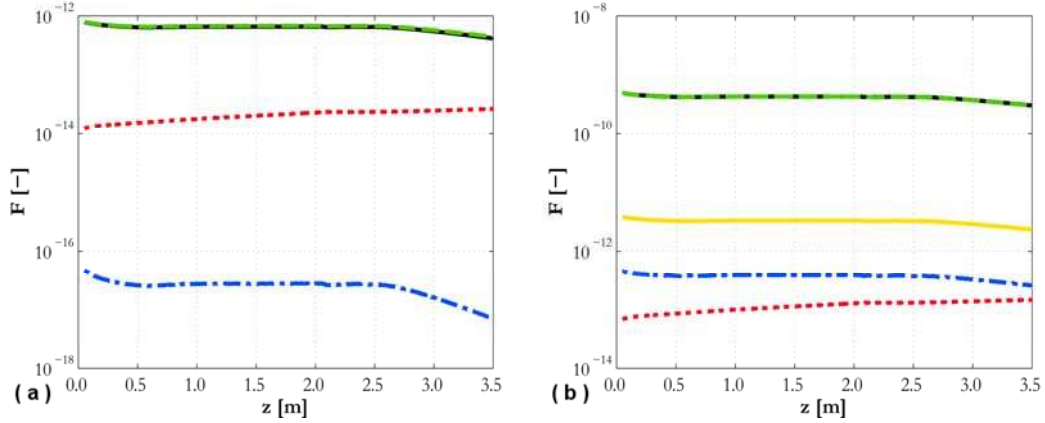


Figure 11. Contribution to force balance in wall-parallel (a) and wall-normal (b) directions for DEBORA experiment (Garnier et al., 2001): (—)  $F_{st}$ ; (— —)  $F_{qsd}$  (a) and  $F_{sl}$  (b); (⋯)  $F_{du}$ ; (— · —)  $F_b$  (a) and  $F_p$  (b); (—)  $F_{cp}$ .

Therefore, and because of the higher surface tension force, when a solution is reached, the bubble departure diameter from Klausner et al. (1993) is significantly higher than that of Yun et al. (2012) and Sugrue and Buongiorno (2016). The latter also both predict a decrease of the departure diameter near the pipe end. An increase in velocity promoted by boiling is expected to increase the effect of drag and lift, which are the main forces promoting bubble departure. In both cases, bubble departure is predicted before lift-off. However, due to uncertainties in the formulation of the drag and lift forces, and in their applicability to the present conditions, additional studies are required.

Preliminary results obtained with subcooling in the Yun et al. (2012) model are considered in Figure 12, which shows the axial wall temperature distribution. In the majority of the region affected by boiling, the liquid in the first cell is superheated. In the first half of the pipe, however, subcooling is significant. Therefore, when the temperature in the first cell is used to evaluate local subcooling, the condensation rate can become so high that a negative bubble diameter is predicted, thus preventing an acceptable solution from being reached. This is due to the use of the temperature in the centre of the near-wall cell, which must be located some distance from the wall. At the pressures of the experiments, the bubbles are much smaller than the near wall cell size, and the temperature in the first cell is not representative of conditions at the bubble cap. Better quantification of the local value of the temperature on the bubble cap is

necessary to account properly for the impact of condensation on bubble departure inside CFD codes.

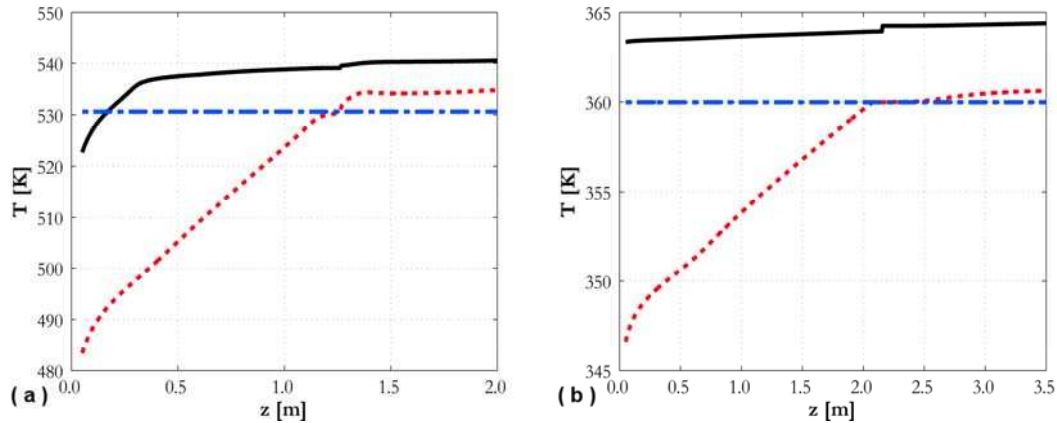


Figure 12. Predicted temperatures in near-wall region for Bartolomei and Chanturiya (1967) (a) and DEBORA (Garnier et al., 2001) (b): (—) wall temperature; (···) liquid temperature in near-wall cell; (- · -) saturation temperature.

## 5. CONCLUSIONS

Three semi-mechanistic models of bubble departure diameter were implemented into the RPI wall heat flux partitioning model in the STAR-CCM+ code. Model predictions were compared against vertically upward subcooled boiling flows of water and refrigerant. The limited applicability of the model proposed by Klausner et al. (1993), which uses a constant contact diameter in the surface tension force, was demonstrated, and the models of Yun et al. (2012) and Sugrue and Buongiorno (2016), where the contact diameter is a fraction of the bubble diameter, were shown to be preferable. With these two models, the importance of a coupled calculation of the bubble departure diameter and frequency for improved predictions and better physical consistency of the boiling model was demonstrated. Given the similar predictions of these two models, both of which are in reasonable agreement with wall temperature and void fraction measurements, no clear distinction between the two can be made based on the conditions studied in this work. On one hand, Yun et al. (2012) has the advantage of accounting for the impact of subcooling on bubble growth, which may become dominant in some flow conditions. On the other hand, the much more extended validation of the Sugrue and Buongiorno (2016) model makes it more robust. More specifically, Yun et al. (2012) validated their model against the DEBORA experiment, whereas Sugrue and Buongiorno (2016) compared against five different



databases and a wide range of fluids, geometries and operating conditions. In addition, the subcooling contribution introduced by Yun et al. (2012) is in need of further improvement. Specifically, excessive condensation resulting in a negative bubble diameter was frequently predicted, because the liquid temperature in the near-wall computational cell was not representative of the local conditions on the bubble cap. Numerous areas for further improvement have been identified. The models predict bubble sliding before lift-off, but the sizes of the surface tension, drag and lift forces, which dominate the force balance, are still uncertain. The general applicability of the models to wall boiling conditions therefore needs to be investigated further. Bubble growth is only a limited part of the whole ebullition cycle and advances in the modelling of the whole cycle, including the contribution of quenching to the total heat flux, are required for more accurate prediction of the bubble departure frequency. Extension of the model from isolated bubble growth to more sustained boiling conditions, including bubble merging and coalescence during growth, is also of interest. Finally, grid-independent methods to predict real local conditions on the bubble cap are required to account for condensation, and these need to be tested in conditions where condensation is expected to be relevant, such as at lower pressures.

## ACKNOWLEDGMENTS

The authors gratefully acknowledge discussions with Dr. Andrew Splawski and Dr. Simon Lo of CD-adapco and the financial support of the EPSRC, in the framework of the UK-India Civil Nuclear Collaboration through grant EP/K007777/1, Thermal Hydraulics for Boiling and Passive Systems, and EP/M018733/1, Grace Time, and Rolls-Royce plc.

## NOMENCLATURE

$A_b$	fraction of the wall surface affected by wall boiling [-]
$a$	thermal diffusivity [ $\text{m}^2 \text{s}^{-1}$ ]
$a_i$	interfacial area concentration [ $\text{m}^2 \text{m}^{-3}$ ]
$C_p$	specific heat at constant pressure [ $\text{J kg}^{-1} \text{K}^{-1}$ ]
$D$	pipe diameter [m]
$d_B$	bubble diameter [m]
$d_{dep}$	bubble departure diameter [m]
$d_{SM}$	Sauter-mean bubble diameter [m]
$d_w$	contact diameter [m]
$F$	force [N]

$f$	bubble departure frequency [ $s^{-1}$ ]
$G$	mass flux [ $kg\ m^{-2}\ s^{-1}$ ]
$G_s$	dimensionless shear rate [-]
$g$	gravitational acceleration [ $m\ s^{-2}$ ]
$h$	heat transfer coefficient [ $W\ m^{-2}\ K^{-1}$ ]
$i_{lv}$	latent heat of vaporization [ $J\ kg^{-1}$ ]
$Ja$	Jacob number [-]
$K_{dry}$	fraction of wall surface in contact with the vapour phase during boiling [-]
$k$	turbulence kinetic energy [ $m^2\ s^{-2}$ ]
$L$	pipe length [m]
$M_\gamma$	$\gamma$ -th moment of the bubble diameter distribution [ $m^\gamma$ ]
$N_A$	active nucleation site density [ $m^{-2}$ ]
$n$	bubble concentration [ $m^{-3}$ ]
$p$	pressure [Pa]
$q$	thermal flux [ $W\ m^{-2}$ ]
$R$	bubble radius [m]
$Re$	bubble Reynolds number [-]
$S_\gamma$	$\gamma$ -th moment of the bubble diameter distribution per cubic metre [ $m^\gamma\ m^{-3}$ ]
$T$	temperature [K]
$T^+$	non-dimensional temperature
$t$	time [s]
$t_w$	waiting time [s]
$U$	velocity [ $m\ s^{-1}$ ]
$u_\tau$	shear velocity [ $m\ s^{-1}$ ]
$We_{cr}$	critical Weber number [-]
$x, y$	spatial coordinates [m]
$y^+$	dimensionless wall distance [-]
$z$	pipe axial coordinate [m]

### ***Greek symbols***

$\alpha$	void fraction [-]
$\alpha_i$	advancing contact angle [rad]
$\beta_i$	receding contact angle [rad]
$\gamma$	bubble inclination angle [rad]
$\varepsilon$	turbulence kinetic energy dissipation rate [ $m^2\ s^{-3}$ ]
$\theta$	heated surface inclination angle [rad]
$\lambda$	thermal conductivity [ $W\ m^{-1}\ K^{-1}$ ]
$\nu$	kinematic viscosity [ $m^2\ s^{-1}$ ]
$\rho$	density [ $kg\ m^{-3}$ ]
$\sigma$	surface tension [ $N\ m^{-1}$ ]

### ***Subscripts***

$b$	buoyancy
$br$	breakup
$cl$	coalescence
$cp$	contact pressure

<i>du</i>	unsteady drag
<i>in</i>	inlet
<i>l</i>	liquid
<i>p</i>	pressure
<i>q</i>	quenching
<i>qsd</i>	quasi-steady drag
<i>sl</i>	shear lift
<i>st</i>	surface tension
<i>v</i>	vapour
<i>w</i>	wall

## ACRONYMS

CFD	Computational Fluid Dynamics
DNB	Departure from Nucleate Boiling
PWR	Pressurized Water Reactor
RPI	Rensselaer Polytechnic Institute
SMD	Sauter-Mean Diameter

## REFERENCES

- Bartolomei, G.G., Chanturiya, V.M., 1967. Experimental study of true void fraction when boiling subcooled water in vertical tubes. *Thermal Engineering* 14, 123-128.
- Bestion, D., 2012. Applicability of two-phase CFD to nuclear reactor thermalhydraulics and elaboration of Best Practice Guidelines. *Nuclear Engineering and Design* 253, 311-321.
- Burns, A.D., Frank, T., Hamill, I., Shi, J.M., 2004. The Favre averaged drag model for turbulent dispersion in Eulerian multi-phase flows. 5<sup>th</sup> International Conference on Multiphase Flows, Yokohama, Japan, May 30 - June 4.
- CD-adapco, 2016. STAR-CCM+<sup>®</sup> Version 10.04 User Guide.
- Cheung, S.C.P., Vahaji, S., Yeoh, G.H., Tu, J.Y., 2014. Modeling subcooled flow boiling in vertical channels at low pressures - Part 1: Assessment of empirical correlations. *International Journal of Heat and Mass Transfer* 75, 736-753.
- Cole, R., 1960. A photographic study of pool boiling in the region of the critical heat flux. *AIChE Journal* 6, 533-538.
- Colombo, M., Fairweather, M., 2015. Prediction of bubble departure in forced convection boiling: A mechanistic model. *International Journal of Heat and Mass Transfer* 85, 135-146.
- Colombo, M., Fairweather, M., 2016a. Accuracy of Eulerian-Eulerian, two-fluid CFD boiling models of subcooled boiling flows. *International Journal of Heat and Mass Transfer* 103, 28-44.
- Colombo, M., Fairweather, M., 2016b. RANS simulation of bubble coalescence and break-up in bubbly two-phase flows. *Chemical Engineering Science* 146, 207-225.
- Cooper, M.G., Lloyd, A.J.P., 1969. The microlayer in nucleate pool boiling. *International Journal of Heat and Mass Transfer* 12, 895-913.
- Del Valle, V.H., Kenning, D.B.R., 1985. Subcooled flow boiling at high heat flux. *International Journal of Heat and Mass Transfer* 28, 1907-1920.
- Forster, H.K., Zuber, N., 1954. Growth of a vapor bubble in a superheated liquid. *Journal of Applied Physics* 25, 474-478.

- Garnier, G., Manon, E., Cubizolles, G., 2001. Local measurements of flow boiling of refrigerant 12 in a vertical tube. *Multiphase Science and Technology* 13, 1-111.
- Gilman, L., Baglietto, E., 2017. A self-consistent, physics-based boiling heat transfer modeling framework for use in computational fluid dynamics. *International Journal of Multiphase Flow* 95, 35-53.
- Hibiki, T., Ishii, M., 2006. Active nucleation site density in boiling systems. *International Journal of Heat and Mass Transfer* 49, 2587-2601.
- Ishii, M., Hibiki, T., 2006. *Thermo-fluid dynamics of two-phase flow*. Springer, New York, USA.
- Jones, W.P., Launder, B.E., 1972. The prediction of laminarization with a two-equation model of turbulence. *International Journal of Heat and Mass Transfer* 15, 301-314.
- Klausner, J.F., Mei, R., Bernhard, D.M., Zeng, L.Z., 1993. Vapor bubble departure in forced convection boiling. *International Journal of Heat and Mass Transfer* 36, 651-662.
- Kocamustafaogullari, G., 1983. Pressure dependence of bubble departure diameter for water. *International Communications in Heat and Mass Transfer* 10, 501-509.
- Koncar, B., Matkovic, M., 2012. Simulation of turbulent boiling flow in a vertical rectangular channel with one heated wall. *Nuclear Engineering and Design* 245, 131-139.
- Krepper, E., Rzehak, R., 2011. CFD for subcooled flow boiling: Simulation of DEBORA experiment *Nuclear Engineering and Design* 241, 3851-3866.
- Krepper, E., Rzehak, R., Lifante, C., Frank, T., 2013. CFD for subcooled flow boiling: coupling wall boiling and population balance models. *Nuclear Engineering and Design* 255, 330-346.
- Kurul, N., Podowski, M.Z., 1990. Multi-dimensional effects in sub-cooled boiling. 9<sup>th</sup> International Heat Transfer Conference, Jerusalem, Israel, August 19-24.
- Lo, S., Zhang, D., 2009. Modelling of break-up and coalescence in bubbly two-phase flows. *Journal of Computational Multiphase Flow* 1, 23-38.
- Mazzocco, T., Ambrosini, W., Kommajosyula, R., Baglietto, E., 2018. A reassessed model for mechanistic prediction of bubble departure and lift off diameters. *International Journal of Heat and Mass Transfer* 117, 119-124.
- Mikic, B.B., Rohsenow, W.M., 1969. A new correlation of pool-boiling data including the effect of heating surface characteristics. *International Journal of Heat and Mass Transfer* 91, 245-250.
- Plesset, M.S., Zwick, S.A., 1954. The growth of vapor bubbles in superheated liquids. *Journal of Applied Physics* 25, 493-500.
- Ranz, W.E., Marshall, W.R., 1952. Evaporation from drops. *Chemical Engineering Progress* 48, 141-146.
- Situ, R., Hibiki, T., Ishii, M., Mori, M., 2005. Bubble lift-off size in forced convective subcooled boiling flow. *International Journal of Heat and Mass Transfer* 48, 5536-5548.
- Sugrue, R., Buongiorno, J., 2016. A modified force-balance model for prediction of bubble departure diameter in subcooled flow boiling. *Nuclear Engineering and Design* 305, 717-722.
- Thakrar, R., Murallidharan, J., Walker, S.P., 2014. An evaluation of the RPI model for the prediction of the wall heat flux partitioning in subcooled boiling flows. 22<sup>nd</sup> International Conference on Nuclear Engineering (ICONE-22), Prague, Czech Republic, July 7-11.
- Thakrar, R., Murallidharan, J., Walker, S.P., 2017. CFD investigation of nucleate boiling in non-circular geometries at high pressure. *Nuclear Engineering and Design* 312, 410-421.
- Thakrar, R., Walker, S.P., 2016. CFD prediction of subcooled boiling flow with semi-mechanistic bubble departure diameter modelling. 25<sup>th</sup> International Conference Nuclear Energy for New Europe (NENE-2016), Portoroz, Slovenia, September 5-8.

- Tolubinsky, V.I., Kostanchuk, D.M., 1970. Vapour bubbles growth rate and heat transfer intensity at subcooled water boiling 4<sup>th</sup> International Heat Transfer Conference, Paris, France.
- Tomiyama, A., Kataoka, I., Zun, I., Sakaguchi, T., 1998. Drag coefficients of single bubbles under normal and micro gravity conditions. *JSME International Journal Series B Fluids and Thermal Engineering* 41, 472-479.
- Wu, W., Chen, P., Jones, B.G., Newell, T.A., 2008. A study of bubble detachment and the impact of the heated surface structure in subcooled nucleate boiling flows. *Nuclear Engineering and Design* 238, 2693-2698.
- Yadigaroglu, G., 2014. CMFD and the critical-heat-flux grand challenge in nuclear thermal-hydraulics. *International Journal of Multiphase Flow* 67, 3-12.
- Yao, W., Morel, C., 2004. Volumetric interfacial area prediction in upward bubbly two-phase flow. *International Journal of Heat and Mass Transfer* 47, 307-328.
- Yeoh, G.H., Tu, J.Y., 2006. Two-fluid and population balance models for subcooled boiling flow. *Applied Mathematical Modelling* 30, 1370-1391.
- Yeoh, G.H., Vahaji, S., Cheung, S.C.P., Tu, J.Y., 2014. Modeling subcooled flow boiling in vertical channels at low pressures - Part 2: Evaluation of mechanistic approach. *International Journal of Heat and Mass Transfer* 75, 754-768.
- Yun, B.J., Splawski, A., Lo, S., Song, C.H., 2012. Prediction of a subcooled boiling flow with advanced two-phase flow models. *Nuclear Engineering and Design* 253, 351-359.
- Zeng, L.Z., Klausner, J.F., Bernhard, D.M., Mei, R., 1993a. A unified model for the prediction of bubble detachment diameters in boiling systems - I. Pool boiling. *International Journal of Heat and Mass Transfer* 36, 2261-2270.
- Zeng, L.Z., Klausner, J.F., Mei, R., 1993b. A unified model for the prediction of bubble detachment diameters in boiling systems- II. Flow boiling. *International Journal of Heat and Mass Transfer* 36, 2271-2279.